Accepted Manuscript

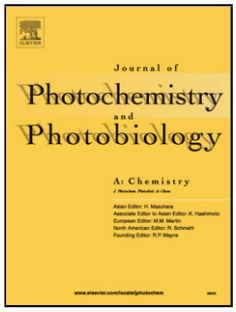

Title: Photodegradation of sulfamethazine, sulfamethoxypiridazine, amitriptyline, and clomipramine drugs in aqueous media

Author: Rania Nassar Aurélien Trivella Samia Mokh Mohamad Al-Iskandarani Hélène Budzinski Patrick Mazellier

PII: S1010-6030(16)30523-8
DOI: http://dx.doi.org/doi:10.1016/j.jphotochem.2016.12.008
Reference: JPC 10463

To appear in: *Journal of Photochemistry and Photobiology A: Chemistry*

Received date: 28-6-2016
Revised date: 29-11-2016
Accepted date: 10-12-2016

Please cite this article as: Rania Nassar, Aurélien Trivella, Samia Mokh, Mohamad Al-Iskandarani, Hélène Budzinski, Patrick Mazellier, Photodegradation of sulfamethazine, sulfamethoxypiridazine, amitriptyline, and clomipramine drugs in aqueous media, Journal of Photochemistry and Photobiology A: Chemistry http://dx.doi.org/10.1016/j.jphotochem.2016.12.008

This is a PDF file of an unedited manuscript that has been accepted for publication. As a service to our customers we are providing this early version of the manuscript. The manuscript will undergo copyediting, typesetting, and review of the resulting proof before it is published in its final form. Please note that during the production process errors may be discovered which could affect the content, and all legal disclaimers that apply to the journal pertain.

ACCEPTED MANUSCRIPT

Photodegradation of sulfamethazine, sulfamethoxypiridazine, amitriptyline, and clomipramine drugs in aqueous media

Rania Nassar[1,2], Aurélien Trivella[3,4], Samia Mokh[2], Mohamad Al-Iskandarani[1,2], Hélène Budzinski[3,4], Patrick Mazellier[3,4*]

[1] Faculty of Public Health I, Lebanese University, Hadath, Lebanon

[2] Laboratory for Analysis of Organic Compound LACO, National Council for Scientific Research CNRS, Lebanese Atomic Energy Commission LAEC, 11‑8281, Riad El Solh, Beirut 1107 2260, Lebanon

[3] University of Bordeaux, EPOC, L'équipe de Physico et Toxico Chimie de l'Environnement, UMR 5805, F 33400 Talence, France

[4] CNRS, EPOC, UMR 5805, F-33400 Talence, France

* Corresponding author: Patrick Mazellier,

ACCEPTED MANUSCRIPT

Highlights

- Irradiation of selected drugs leads to the formation of several photoproducts
- The methoxy substituent is at the origin of the bathochromic shift which allows absorption up to 380 nm for SMP while no absorption is observed above 350 nm for SMT
- No degradation was observed for amitriptyline
- Photosensitizers enhanced the degradation of amitriptyline and clomipramine in river water

Abstract

The photochemical transformation of two antibacterial sulfonamides, namely sulfamethazine (SMT) and sulfamethoxypyridazine (SMP), and two tricyclic antidepressants, namely amitriptyline (AMT) and clomipramine (CMP) were investigated. Experiments conducted in river water under artificial sunlight irradiation show an acceleration of the degradation for SMT, SMP, and CMP of a factor 1.6 to 7.7 by comparison to purified water. This acceleration is, at least partially, due to photosensitized reactions which can occur in river water. The photodegradation of CMP was particularly fast. In addition, no degradation was observed for AMT in purified water while photosensitized reaction occurs. Under ultra-violet (254 nm) irradiation in purified water, the four drugs were degraded. Calculated quantum yields of photodegradation were of 4.3×10^{-3}, 5.1×10^{-3}, 7.6×10^{-3}, and 65.0×10^{-3} respectively for SMT, SMP, AMT, and CMP. UV coupled with hydrogen peroxide (UV/H_2O_2) was used as an advanced

ACCEPTED MANUSCRIPT

oxidation process for water depollution. The calculated second order rate constants of reaction with hydroxyl radicals were of $5.0x10^9$, $5.0x10^9$, $8.0x10^9$ and $9.5x10^9$ L mol^{-1} s^{-1} for SMT, SMP, AMT and CMP, respectively. Finally, the structures of photoproducts were proposed according to LC-MS/MS analyses. The elimination of SO_2 was the main photochemical process for SMT and SMP. In the case of AMT and CMP, hydration and hydroxylation, respectively, were observed.

Keywords: antibacterial sulfonamides, tricyclic antidepressant, photodegradation, artificial sunlight, UV irradiation.

1. Introduction

Medicine residues are organic micropollutants of great interest due to their extensive use and their increasing occurrence in the aquatic environment [1]. These residues potentially impact water quality, ecosystems, and human health [2]. Some of these pharmaceutical compounds are not completely removed by waste water treatment plants [3,4]. Drugs most frequently found in wastewater are antibiotics, antacids, steroids, antidepressants, analgesics, anti-inflammatories, antipyretics, beta-blockers, lipid-lowering drugs, tranquilizers, and stimulants [5]. Potential health effects and acute toxicity of those micropollutants are not always well known. For example, one of the major concerns of antibiotic residues in the environment involves the development of resistant bacteria [6]. Polluted water can generally be treated efficiently by biological treatment plants, and by using adsorbents or conventional chemical treatments (chlorination, ozonation …). However, these procedures are occasionally not able

ACCEPTED MANUSCRIPT

to degrade pollutants to the levels required by law or essential for the subsequent use of the effluent [3].

Ultraviolet (UV) treatment of water is being used for disinfection of wastewater and drinking water in North America, Europe, and numerous countries around the world [1]. This technique is very effective in advanced water treatment technologies [7]. Furthermore, advanced oxidation processes, in particular UV irradiation coupled with hydrogen peroxide (UV/H_2O_2), are very effective in the oxidation of numerous organic and inorganic compounds [8]. These processes are all based on the generation of highly reactive free radicals ($HO^{\bullet}$, $O_2^{\bullet -}$, $HO_2^{\bullet}$) [9-11]. During UV/H_2O_2 treatment, oxidation occurs mainly by $HO^{\bullet}$ radicals which react unselectively with organic contaminants. Second order reaction rate constants in the order of 10^8-10^{10} L mol^{-1} s^{-1} have been reported for many organic compounds [12].

The aims of the present study were to evaluate the photodegradation kinetic constants of sulfamethazine (SMT), sulfamethoxypyridazine (SMP), amitriptyline (AMT), and clomipramine (CMP) antibiotic and antidepressant compounds by irradiating them in different water matrices by means of simulated sunlight and a UV source (254 nm) alone or coupled with hydrogen peroxide. Quantum yields of direct photodegradation were also calculated for the four compounds under a 254 nm irradiation. Pharmaceutical compounds SMT and SMP were chosen due to their massive use in veterinary medicine [13]. AMT and CMP drugs were chosen for their use in human medicine [14]. Their presence in ground [15], surface [16,17] and drinking [18] waters was reported. Finally, the structural characterization of the degradation products formed during UV irradiation was performed by means of LC-MS/MS analyses.

ACCEPTED MANUSCRIPT

2. Materials and methods

2.1 Chemicals

High purity standards of sulfamethazine (SMT, ≥ 99 %), sulfamethoxypyridazine (SMP, ≥ 97 %), amitriptyline (AMT, ≥ 98 %), clomipramine (CMP, ≥ 98 %), and hydrogen peroxide (30%, w/w) were purchased from Sigma-Aldrich.

HPLC grade solvents (water, methanol - MeOH, and acetonitrile - ACN) were supplied from Sigma-Aldrich. For each drug, stock solutions were prepared at a concentration of 100 mg L^{-1} in purified water using a Millipore device (resistivity 18.2 MΩ cm, DOC < 0.1 mg L^{-1}). The solutions were stored in dark at 4 °C until use. All the experiments have been performed at pH 6.1.

River water was sampled three times from the "Isle" in Périgueux (France) in July 2012, May 2013 and May 2014 (7.8 < pH < 8.0; total organic carbon (TOC): 0.2 mg L^{-1}). The river water was filtered with a 0.45 µm membrane prior to use for photochemical experiments. One liter of the river water was acidified with 5 mL of sulfuric acid (7.5 M) for measurement of the permanganate index (6.2, 3.1 and 2.5 mg O_2 L^{-1} in July 2012, and May 2013 and 2014).

Drug concentrations used for photodegradation kinetics and photoproducts identification experiments were in the range 0.3-0.5 µmol L^{-1} and 30-35 µmol L^{-1}, respectively.

2.2 UV-Visible spectroscopy

UV-Vis spectra were recorded on a Shimadzu double-beam spectrophotometer (UV-1800), using either 1 or 5 cm quartz cells (Hellma Analytics, QS). Baselines (purified water) and spectra were recorded at room temperature with a 1-nm resolution.

Molar absorption coefficients of each drug were calculated using solutions with concentrations ranging from 1.8 µM to 5.6 µM. Absorbance of solutions were measured using a 1-cm cell.

2.3 LC-UV and LC-MS/MS analyses

ACCEPTED MANUSCRIPT

The concentration of target drugs at different irradiation times was quantified by liquid chromatography (Agilent, 1100 series) coupled with UV detection (LC-UV). UV absorption of SMT and SMP was recorded at 260 nm, that of AMT at 240 nm, and that of CMP at 230 nm. A Nucleosil C_{18} 5 µm-100 Å column (250 mm × 4.6 mm) was used for SMT and SMP analyses. A Nucleosil C_{18} Nautilus column (same packing material) was used for AMT and CMP analyses. The flow rate was set to 1 mL min^{-1}. Solvent A was MeOH and solvent B purified water. SMT and SMP analyses were performed from a mobile phase composed of 65% of A. In the case of AMT and CMP analyses, the mobile phase was prepared from 50% of A and 50% of B adjusted to pH 3 by adding 10 mM of formic acid. All the experiments were performed in isocratic mode. The sample injection volume was set to 20 µL for SMT and SMP, and to 50 µL for AMT and CMP.

The structural identification of photoproducts was carried out with an Agilent 1200 LC system (Agilent Technologies, USA) coupled to an Agilent 6410 triple quadrupole mass spectrometer (LC-MS/MS). The eluents and columns used for the separation of the parent compound and its photoproducts were the same as those of LC-UV analyses. The flow rate was set to 0.6 mL min^{-1}. Detection was performed with an electrospray ionization (ESI) source operating in positive mode. The following conditions were set: source temperature 450 °C, capillary voltage 3000 V. The collision energy was adjusted from 5 to 30 V to obtain the fragmentation patterns when performing product ion scans. Nitrogen was used as collision gas and nebulization gas at 30 and 40 psi, respectively.

2.4 Irradiation experiments

UV irradiation (254 nm) experiments were performed in purified water. The irradiation setup was a batch photoreactor (volume of irradiated solution: 2 L, optical path length: 3.6 cm). The lamp (Vilber-Lourmat T6C-254 nm, low pressure Hg lamp 6 W) was located at the center of the reactor, in a quartz sleeve. The photon fluence rate (I_0) was evaluated by hydrogen

ACCEPTED MANUSCRIPT

peroxide actinometry [19]. A value of $1.36x10^{-6}$ E L^{-1} s^{-1} was obtained. Hydrogen peroxide concentration was measured by the Ti-complexometry method described by Eisenberg [20].

Simulation of natural sunlight was carried out using a Suntest CPS instrument from Atlas Material Testing Technology (Chicago, Illinois, USA), equipped with a xenon arc lamp and UV-IR filters ($\lambda \geq 290$ nm). The emitted UV-Visible wavelengths ranged from 290 to 800 nm. Irradiance was set to 250 W m^{-2}. Drug solutions were prepared in purified and river waters and transferred into 12 mL glass tubes (optical pathlength: 1.5 cm). Before irradiation, aliquots of 1 mL of each spiked sample were taken off and stored in the dark (aluminum wrapped vials) at room temperature (26 °C). For dark control experiments, non-irradiated samples were wrapped in aluminum foil and dropped off into the sample compartment in the same conditions than unwrapped samples. Drugs were irradiated in the Suntest over a period of 7 hours. Aliquots of 1 mL were withdrawn for analysis at scheduled time intervals.

2.4 Reaction rate constants and photodegradation quantum yields

2.4.1 Direct photolysis

The degradation pattern of target drugs (D) was adjusted to the pseudo-first order kinetic model, which assumes a decrease of the concentration through time proportional to the concentration remaining in the matrix. The model follows equation (1):

$$\ln([D]/[D]_0) = - k_{app}\, t \quad (1)$$

where $[D]_0$ and [D] are the drug concentrations (mol L^{-1}) respectively before and during irradiation, k_{app} is the apparent first order reaction rate constant (s^{-1}), and t is the irradiation time (s).

Aqueous solutions of target drugs ($0.3 \leq [D] \leq 0.8$ µmol L^{-1}) were irradiated at 254 nm. A disappearance of the organic compound is observed according to the reaction:

$$D \xrightarrow{h\nu} \text{degradation products} \qquad \text{with } -d[D]/dt = \phi_{(D)}\ I_0(1-10^{-A}) \qquad (2)$$

ACCEPTED MANUSCRIPT

where $\phi_{(D)}$ is the quantum yield of degradation at 254 nm, I_0 is the photon fluence rate of the irradiation source ($I_0 = 1.36 \times 10^{-6}$ E L^{-1} s^{-1}), and A is the absorbance at 254 nm.

Working concentrations were chosen such as the absorbance at 254 nm is lower than 0.02 (hyper dilute medium). Thus, the rate of photodegradation of D can be simplified from (2) to (3):

$$-d[D]/dt = 2.303\ A\ \phi_{(D)}\ I_0 \qquad (3)$$

Eq. (3) indicates that the photodegradation of D follows to an apparent first order kinetics law. Thus, the expression of the monochromatic quantum yield is:

$$\phi_{(D)} = k_{app} / (2.303\ I_0\ \varepsilon_D\ \ell) \qquad (4)$$

where $\phi_{(D)}$ is the quantum yield of degradation at 254 nm, k_{app} is the apparent first order reaction rate constant (s^{-1}), I_0 is the photon fluence rate of the irradiation source, ε_D is the molar absorption coefficient of the drug at 254 nm, and ℓ is the internal radius of the reactor minus the radius of the monochromatic lamp (the UV source was placed at the center of the reactor).

2.4.2 **Photosensitized reactions**.

The UV irradiation (λ = 254 nm) of hydrogen peroxide in aqueous solution leads to the production of hydroxyl radicals ($HO^\bullet$) following the reaction:

$$H_2O_2 \xrightarrow{h\nu} 2\ HO^\bullet \quad \text{with } d[HO^\bullet]/dt = 2\ \phi_{H2O2}\ I_a \qquad (5)$$

where $-d[HO^\bullet]/dt$ is the rate of formation of $HO^\bullet$ radicals (mol L^{-1} s^{-1}), ϕ_{H2O2} is the hydrogen peroxide quantum yield of photodegradation at 254 nm (ϕ_{H2O2} = 0.5, [21]), and I_a is the rate of light absorption (E L^{-1} s^{-1}).

Aqueous solutions of D were irradiated in the presence of large amounts of hydrogen peroxide ($[H_2O_2]_0$ = 0.05, 0.08, 0.10 and 0.20 mol L^{-1}) at 254 nm. No change in D concentration was observed in the presence of such excess of hydrogen peroxide but in the absence of UV light meaning that no dark reaction occurred. In the time scale of experiments,

ACCEPTED MANUSCRIPT

the concentration of hydrogen peroxide was shown to remain almost constant: $[H_2O_2]_t$ / $[H_2O_2]_0 > 0.98$. Under UV irradiation the following reactions occur:

$HO^\bullet + H_2O_2 \xrightarrow{k_{H2O2}} HO_2^\bullet + H_2O$ $\quad -d[H_2O_2]/dt = k_{H2O2}\,[H_2O_2]\,[HO^\bullet]$ (6)

$HO^\bullet + D \xrightarrow{k_D}$ degradation products $\quad -d[D]/dt = k_D\,[D]\,[HO^\bullet]$ (7)

At a given time, the steady-state concentration of hydroxyl radicals is given by the Eq. 8:

$$[HO^\bullet] = (2\,\phi_{H2O2} \times I_a) / (k_{H2O2}[H_2O_2]_0 + k_D\,[D]_0) \quad (8)$$

where $[HO^\bullet]$ is the hydroxyl radical concentration (mol L^{-1}), I_a is the rate of light absorption (E L^{-1} s^{-1}), k_{H2O2} is the second order rate constant of reaction of hydrogen peroxide with hydroxyl radicals ($k_{H2O2} = 2.7\times10^7$ L mol^{-1} s^{-1}, [21]), $[H_2O_2]_0$ is the concentration of hydrogen peroxide before irradiation (mol L^{-1}), k_D is the second order rate constant of reaction of the drug with hydroxyl radicals (L mol^{-1} s^{-1}), and $[D]_0$ is the concentration of the drug before irradiation (mol L^{-1}).

Reactions of $HO_2^\bullet$ with D can be neglected in our conditions due to the well-known lower reactivity of this radical compared to $HO^\bullet$ radicals.

If hydrogen peroxide concentration is high enough ($A_{254nm} > 2$), it is considered that the incident light is completely absorbed by hydrogen peroxide. Moreover, the decrease in H_2O_2 concentration is low (< 5%) in the time scale of the experiments and $k_{H2O2}\,[H_2O_2]_0 >> k_D\,[D]_0$ even if a value of k_D of 10^{10} is considered. Then, the expression of Eq. 8 can be simplified:

$$[HO^\bullet] = 2\,\phi_{H2O2} \times I_0 / (k_{H2O2}\,[H_2O_2]_0) \quad (9)$$

The D disappearance as a function of time can be written according to relations 7 and 9:

$$-\ln([D]/[D]_0) = 2\,k_D\,\phi_{H2O2}\,I_0\,t / (k_{H2O2}\,[H_2O_2]_0) \quad (10)$$

The plot of $\ln([D]/[D]_0)$ as a function of reaction time allows the determination of the second order rate constant of reaction between the drug and hydroxyl radicals (k_D).

ACCEPTED MANUSCRIPT

3. Results and discussion

3.1 UV-Vis absorption spectra

Fig. 1 shows the UV-Vis absorption spectra of sulfamethazine (SMT), sulfamethoxypyridazine (SMP), amitriptyline (AMT) and clomipramine (CMP) in aqueous solutions at pH 6.1. UV-Vis spectra display maxima at 240 ($1.7x10^4$ L mol^{-1} cm^{-1}) and 263 nm ($1.8x10^4$ L mol^{-1} cm^{-1}) for SMT, and 263 nm ($1.8x10^4$ L mol^{-1} cm^{-1}) for SMP (Fig. 1a). SMT and SMP have a common absorption maximum at 263 nm due to their structural similarities, especially the substituted benzene cycle which is present in both structures. Differences can be observed from the pyrimidine (SMT) and pyridazine (SMP) cycles and the nature of their substituents. In particular, the methoxy group is at the origin of a bathochromic shift of the $\pi \rightarrow \pi^*$ transition of the substituted pyridazine cycle [22,23] and this one allows absorption up to 380 nm for SMP while no absorption is observed above 350 nm for SMT. UV-Vis absorption spectra of AMT and CMP are totally different despite their structural similarities (Fig. 1b). Maxima of absorption are located at 210 ($3.5x10^4$ L mol^{-1} cm^{-1}) and 240 nm ($1.2x10^4$ L mol^{-1} cm^{-1}) for AMT, and 220 ($2.1x10^4$ L mol^{-1} cm^{-1}), 253 ($6.8x10^3$ L mol^{-1} cm^{-1}) and 280 nm ($5.8x10^3$ L mol^{-1} cm^{-1}) for CMP. Moreover, AMT do not absorb above 290 nm while CMP absorbs light up to 320 nm. These spectral differences can be explained by the presence of a chlorine atom and especially a nitrogen atom located in the CMP tricyclic part which induce $n \rightarrow \pi^*$ transitions. In addition, the heteroatoms are responsible for bathochromic shifts of the $\pi \rightarrow \pi^*$ bands. To a lesser extent, the increase conjugation in the AMT structure also induced a bathochromic shift of the $\pi \rightarrow \pi^*$ transitions.

3.2 Kinetic data and quantum yields

Kinetic data and quantum yields obtained under simulated solar light and UV irradiation are gathered in Table 1. The photodegradation of SMT, SMP, AMT and CMP under artificial sunlight irradiation was studied in purified and river waters. SMT, SMP and CMP

ACCEPTED MANUSCRIPT

decomposition followed a pseudo-first order kinetics in the two aqueous matrices while AMT was not degraded after seven hours of irradiation in purified water. This latter result is in line with the absence of absorption above 290 nm on the UV-Vis spectrum of AMT (Fig. 1b). For the same duration of irradiation, AMT was not degraded in the river water. SMT and SMP degradation rate constants measured in purified water were respectively of $1.1x10^{-3}$ and $0.9x10^{-3}$ min^{-1}. The two sulfonamides disappeared with comparable kinetics upon irradiation under the used lamp.CMP degradation was fast by comparison with sulfonamides. The degradation rate constant was of $18.2x10^{-3}$ min^{-1}. In river water, an increase of the rate constants was observed for the three degraded drugs. The photochemical transformation of SMP ($k_R = 6.9x10^{-3}$ min^{-1}) was 1.9 fold faster than that of SMT ($k_R = 3.7x10^{-3}$ min^{-1}). The observed differences between the two aqueous media can be assigned not only to the presence of photosensitizers in river water [24] but also to the change of protonation state (SMT: pK_{a1} = 2.8 and pK_{a2} = 7.0, and SMP: pK_{a1} = 2.2 and pK_{a2} = 7.3). In fact, the experiments were carried out in purified water at pH 6.1 and in river water at pH 7.8. The change in protonation state of the sulfonamide compounds can induce modifications of UV-Vis absorption and could be, at least partially, at the origin of the acceleration of the degradation. In 2011, Baeza and Knappe [25] studied the effect of pH on SMT photolysis rate and the results show that the anionic form photolyzed more rapidly than the neutral one. The quantum yield values were calculated at 254 nm to be 2.8×10^{-3}, 8.7×10^{-3} and 8.4×10^{-3} respectively at pH 3.6, 7.85 and 9.7. In 2012, García-Galán et al. [26] reported the behavior of SMT under artificial solar light irradiation in both purified water and in reclaimed wastewater, in order to compare the influence of dissolved organic matter. First order rate constants of 1.8×10^{-3} and 2.3×10^{-3} min^{-1} were determined in purified water and waste water, respectively. García-Galán et al. explained that dissolved organic matter contained in the matrix could have acted as a catalyst for this sulfonamide compound. The photolysis kinetics of SMP was evaluated by Khaleel et

ACCEPTED MANUSCRIPT

al. [16]. The first order rate constant was determined in purified water to be 52×10^{-3} min^{-1}, *i.e.* 58 fold higher than that determined in our study. This difference can be explained by the use of a medium-pressure mercury lamp as irradiation source. AMT was persistent after 7 hours of irradiation in river water but 50% of degradation was obtained after 2 days of irradiation (data not shown). CMP degradation rate constant was evaluated as $28.9x10^{-3}$ min^{-1}, almost 2 times higher than in purified water. In the case of AMT (pK_a = 9.41) and CMP (pK_a = 9.28), only neutral forms are present in both aqueous matrices, thus we can confirm that photosensitizers have enhanced their degradation in river water.

Under 254 nm irradiation, the degradation of the four drugs was observed in purified water. The quantum yields were of $4.3x10^{-3}$, $5.1x10^{-3}$, $7.6x10^{-3}$, and $65.0x10^{-3}$ for SMT, SMP, AMT and CMP, respectively (Table 1). The photoreaction efficiency is close for SMT and SMP drugs while a factor 8.6 separates the values obtained for AMT and CMP. Following irradiation at 254 nm, the pseudo-first order rate constants of degradation were of $57.3x10^{-3}$ and $66.0x10^{-3}$ min^{-1} for SMT and SMP, respectively. In the case of AMT and CMP the constants were of $39.9x10^{-3}$ and $367.8x10^{-3}$ min^{-1}. Among the four drugs, a significantly faster degradation of CMP was observed. This result was also obtained from simulated solar light irradiation experiments. This difference can be explained by the lone-pairs of electrons of the chlorine atom. Indeed, this atom has a mesomeric effect which allows to release the electron-pairs to participate to the conjugation with the π electrons of the benzene ring. This effect could enhance the photolytic reactivity of CMP as explained by Lian et al. [27] in the case of sulfachloropyridazine. The photochemical transformation of AMT at a concentration of 1 µmol L^{-1} was investigated in ultrapure water at 20°C using a low pressure mercury lamp (λ = 254 nm) by Real et al. [28]. The value obtained for the quantum yield was close to our value.

In the framework of water depollution, the UV/H_2O_2 advanced oxidation process was used. The selected drugs were oxidized using ultraviolet coupled to hydrogen peroxide at

ACCEPTED MANUSCRIPT

concentrations ranging from 0.03 to 0.20 mol L^{-1}. The calculated second order rate constants were of $5.0x10^9$, $5.0x10^9$, $8.0x10^9$, and $9.5x10^9$ L mol^{-1} s^{-1} for SMT, SMP, AMT and CMP, respectively (Table 1). The presence of H_2O_2 enhanced the degradation rates. This effect is attributed to the photodegradation of H_2O_2, which generates hydroxyl radicals which can oxidize drugs. The second order rate constants (k_D) are in the same order of magnitude with those reported previously for other pharmaceutical compounds [18, 28]. The effects of pH and H_2O_2 concentration on SMT degradation was evaluated by Beaza and Knappe [25], pH affected direct photolysis rates but had little effect on the hydroxyl radical oxidation rate. In fact, k_D value obtained in this study was of 5.6×10^9 L mol^{-1} s^{-1} at pH 7.85 which is similar to that obtained in our study (5.0×10^9 L mol^{-1} s^{-1}) at pH 6.1.

3.3 Photoproduct structures identification

Irradiation of the drugs at 254 nm in the absence of hydrogen peroxide leads to the formation of several photoproducts. The evolution of the concentration of the parent compounds and of photoproducts peak areas as a function of irradiation time are displayed Fig. 2. The sulfonamide drugs yield to the formation of four photoproducts from SMT and two photoproducts from SMP. Three photoproducts are observed from AMT and one from CMP.

LC-MS/MS analyses were performed in positive mode and results are gathered in Table 2. Photodegradation of SMT produced 4 major photoproducts; SMT-1 and SMT-2 with the same m/z (215), and SMT-3 and SMT-4 with m/z of 124.1 and 295.1, respectively (Table 2). The photoproducts are more polar than SMT except SMT-2 (Figure 2). SMT-1 and SMT-2 are formed just at the beginning of the reaction while SMT-3 and SMT-4 start appearing after few minutes of irradiation. The maximal peaks area of the four photoproducts are obtained after 70 minutes of irradiation. The determined elemental composition for SMT-1 and SMT-2 was $C_{12}H_{15}N_4$. These compounds are formed from SO_2 elimination which is the main photochemical transformation process. On the basis of the MS/MS fragmentation patterns, the

ACCEPTED MANUSCRIPT

structures of SMT-1 and SMT-2 were proposed (Scheme 1). The SMT-3 photoproduct is constituted of the pyrimidine part of SMT but can also be formed from the SMT-2 product. The corresponding elemental composition was assigned to $C_6H_{10}N_3$ which would correspond to 4,6-dimethylpyrimidine-2-amine. This structure was found by García Galán et al. [28]. Finally, SMT-4 is issued from the hydroxylation of SMT. The hydroxyl group was located on the benzene cycle due to the formation of the 186 fragment which corresponds to the SO_2-NH-$C_6H_7N_2$ moiety. Similarly, SMT-4 was detected in the study with the fungus T. versicolor [29] verified by the transition 295→108.

During SMP degradation, photoproducts show m/z of 215.0 (SMP-1), 216.1 (SMP-2) and 126.0 (SMP-3). SMP-1 is more polar than SMP and reached its maximal area after 50 minutes of irradiation while SMP-2 is less polar than the parent compound and reached its maximal area after about 150 minutes of irradiation. SMP-1 ($C_{11}H_{11}N_4O$) arises after extraction of SO_2 then elimination of H_2 from the parent drug. The compound lost CH_3OH (-32) to give a fragment at m/z 183. Two alternative structures were proposed on this basis (Scheme 2). The fragmentation pattern of SMP-2 (m/z=216, $C_{11}H_{12}N_4O$) was not helpful to identify its structure. The structure of SMP-3, detected in LC-MS experiments only, corresponds to 4-methoxy-2-amino pyrimidine with a m/z of 126.0. The structure was proposed by Chuang et al. [30].

Photochemical transformation of AMT produced 3 major products upon irradiation at 254 nm, AMT-1 with a m/z of 296.1, AMT-2 and AMT-3 with m/z of 314.2. The photoreactivity of AMT is associated to successive hydrations leading to +18 for AMT-1 ($C_{20}H_{28}NO$) and then +36 for AMT-2 and AMT-3 ($C_{20}H_{28}NO_2$). The fragmentation spectra do not give information allowing the localization of the positions of the OH groups. Benitez et al. proposed a photoproduct structure in the case of nortriptyline hydration which has a similar structure to

ACCEPTED MANUSCRIPT

AMT [31]. Thehydration reaction was located on the unsaturation of the lateral chain. On this basis, structures were proposed for the photoproducts of AMT (Scheme 3).

The photodegradation of CMP leads to only one product (CMP-1, m/z = 297.2). This compound, which is more polar than CMP, appeared from the first minute of reaction and reached its maximal area after 5 minutes. CMP-1 ($C_{20}H_{25}N_2O$) is generated from a nucleophilic substitution reaction, *i.e.* the chlorine atom was replaced by an OH group. This hypothesis is confirmed by the degradation pattern.

4. Conclusion

The photodegradation of SMT, SMP, AMT and CMP was investigated in purified and river water under simulated solar light irradiation in order to evaluate their environmental fate in surface water. It has been demonstrated that SMT and SMP were partially degraded after seven hours of irradiation while CMP degradation was especially fast due to the presence of the chlorine atom. At the opposite, AMT shows no light absorption above 290 nm and thus was not degraded in purified water. Its photosensitized degradation was observed in river water. The presence and persistence of these contaminants in surface water constitute a potential risk for human health. For example, the antibiotics may lead to antibacterial resistance, a threat to public health worldwide.

The four drugs were irradiated at 254 nm and their photoproducts were identified. The results showed that UV water treatment was effective to degrade these drugs basing to the rate constant values, however their degradation yielded several photoproducts with unknown toxicity. LC-MS/MS analyses allowed to identify the photoproduct structures generated under UV irradiation in purified water. The results showed that SMT and SMP have a common pathway of degradation. Their photoproducts were formed after SO_2 elimination. However, the hydroxylated product was observed from SMT degradation only. In the case of AMT and

ACCEPTED MANUSCRIPT

CMP, photo-oxidation processes were observed but the involved mechanisms were different due to the presence of a chlorine atom in the CMP structure and unsaturation on the lateral chain of AMT. Finally, the advanced oxidation process UV/H_2O_2 leaded to complete degradation of the drugs, however a toxicity study will help to confirm that this process could be used for water decontamination.

ACKNOWLEDGEMENTS

The collaboration of the UMR EPOC-LPTC from France, the Laboratory for Analysis of Organic Compound (LACO), and the Lebanese Atomic Energy Commission LAEC (LACO-CLEA) from Lebanon is gratefully acknowledged. Thanks also go to Dr. Ahmad Rifaei for his information in LC-MS/MS analysis and to Prof. Dr. Bilal Nsouli for his support. This study also benefitted from supports from the French National Research Agency (ANR) as part of the Investments for the Future Program, within the Cluster of Excellence COTE (ANR-10-LABX-45).

Appendix A. Supplementary data

Supplementary data associated with this article can be found, in the online version, at

ACCEPTED MANUSCRIPT

REFERENCES

[1] D. Avisar, Y. Lester, H. Mamane, pH induced polychromatic UV treatment for the removal of a mixture of SMX, OTC and CIP from water, J. Hazard Mater. 175 (2010) 1068–1074.

[2] F. Yuan, C. Hu, X. Hu, J. Qu, M. Yang, Degradation of selected pharmaceuticals in aqueous solution with UV and UV/H_2O_2, Water Res. 43 (2009) 1766–1774.

[3] G. R. Boyd, H. Reemtsma, D. A. Grimm, S. Mitra, Pharmaceuticals and personal care products (PPCPs) in surface and treated waters of Louisiana, USA and Ontario, Canada, Sci. Total Environ. 311 (2003) 135–149.

[4] T. Heberer, Tracking persistent pharmaceutical residues from municipal sewage to drinking water, J. Hydrol. 266 (2002) 175–189.

[5] J. Rivera-Utrilla, M. Sánchez-Polo, M. Á. Ferro-García, G. Prados-Joya, R. Ocampo-Pérez, Pharmaceuticals as emerging contaminants and their removal from water. A review, Chemosphere 93 (2013) 1268–1287.

[6] V. Homem, L. Santos, Degradation and removal methods of antibiotics from aqueous matrices–A review, J. Environ. Manage. 92 (2011) 2304–2347.

[7] F. J. Benitez, J. L. Acero, F. J. Real, G. Roldan, E. Rodriguez, Photochemical transformation of model emerging contaminants in ultra-pure water: Kinetics, by-products formation and degradation pathways, Water Res. 47 (2013) 870–880.

[8] O. Legrini, E. Oliveros, A. M. Braun, Photochemical processes for water treatment, Chem. Rev. 93 (1993) 671–698.

[9] S. Esplugas, D. M. Bila, L. G. T. Krause, M. Dezotti, Ozonation and advanced oxidation technologies to remove endocrine disrupting chemicals (EDCs) and pharmaceuticals and personal care products (PPCPs) in water effluents, J. Hazard. Mater. 149 (2007) 631–642.

ACCEPTED MANUSCRIPT

[10] S. Baumgarten, H. F. Schröder, C. Charwath, M. Lange, S. Beier, J. Pinnekamp, Evaluation of advanced treatment technologies for the elimination of pharmaceutical compounds, Water Sci. Technol. 56 (2007) 1–8.

[11] C. Von Sonntag, Advanced oxidation processes: mechanistic aspects, Water Sci. Technol. 58 (2008) 1015-1021.

[12] F. L. Rosario-Ortiz, E. C. Wert, S. A. Snyder, Evaluation of UV/H_2O_2 treatment for the oxidation of pharmaceuticals in wastewater, Water Res. 44 (2010) 1440–1448.

[13] E. P. Tolika, V. F. Samanidou, I. N. Papadoyannis, Development and validation of an HPLC method for the determination of ten sulfonamide residues in milk according to 2002/657/EC., J. Sep. Sci. 34 (2011) 1627–1635.

[14] J. L. F. C. Limaa, J. A. V. Prior, B. F. Reis, J. L. M. Santos, E. A. G. Zagatto, Automated spectrophotometric determination of clomipramine on a multicommutated flow system, Anal. Chim. Acta 467 (2002) 75–81.

[15] G. Hamscher, H. T. Pawelzick, H. Hoper, H. Nau, Different behavior of tetracyclines and sulfonamides in sandy soilsafter repeated fertilisation with liquid manure, Environ. Toxicol. Chem. 24 (2005) 861–868.

[16] N. D. Khaleel, W. M. Mahmoud, G. M. Hadad, R. A. Abdel-Salam, K. Kümmerer, Photochemical transformation of sulfaméthoxypyridazine in various aqueous media: Aerobic biodegradation and identification of photoproducts by LC-UV–MS/MS, J. Hazard Mater. 244–245 (2013) 654– 661.

[17] J. Giebułtowicz, G. Nałęcz-Jawecki, Occurrence of antidepressant residues in the sewage-impacted Vistula and Utrata rivers and in tap water in Warsaw (Poland), Ecotoxicol. Environ. Saf. 104 (2014) 103–109.

ACCEPTED MANUSCRIPT

[18] M. C. Dodd, M. O. Buffle, U. Von Gunten, Oxidation of antibacterial molecules by aqueous ozone: moiety-specific reaction kinetics and application to ozone-based wastewater treatment, Environ. Sci. Technol. 40 (2006) 1969–1977.

[19] I. Nicole, J. De Laat, M. Dore, J. P. Duguet, C. Bonnell, Use of UV radiation in water treatment measurement of photonic flux hydrogen peroxide actinometry, Water Res. 24 (1990) 157−168.

[20] G. M. Eisenberg, Colorimetric Determination of Hydrogen Peroxide, Ind. Eng. Chem. Anal. Ed. 15 (1943) 327–328.

[21] P. Mazellier, A. Rachel, V. Mambo, Kinetics of benzenesulfonates elimination by UV and UV/H_2O_2, J. Photoch. Photobio. A 163 (2004) 389–393.

[22] R. B. Woodward, Structure and Absoprtion Spectra. III. Normal Conjugated Dienes, J. Am. Chem. Soc. 64 (1942). 72-75.

[23] L. F. Fieser, M. Fieser, S. Rajagopalan, Absorption spectroscopy and the structures of the diosterols, J. Org. Chem. 13 (1948) 800-806.

[24] P. C. Rua-Gómez, W. Püttmann, Degradation of lidocaine, tramadol, venlafaxine and the metabolites O-desmethyltramadol and O-desmethylvenlafaxine in surface waters, Chemosphere 90 (2013) 1952-1959.

[25] C. Baeza, D. R. U. Knappe, Transformation kinetics of biochemically active compounds in low-pressure UV Photochemical transformation and UV/H_2O_2 advanced oxidation processes, Water Res. 45 (2011) 4531–4543.

[26] M. J. García-Galán, M. S. Díaz–Cruz, D. Barceló, Kinetic studies and characterization of photolytic products of sulfaméthazine, sulfapyridine and their acetylated metabolites in water under simulated solar irradiation, Water Res. 46 (2012) 711–722.

ACCEPTED MANUSCRIPT

[27] J. Lian, Z. Qiang , M. Li , J. R. Bolton, J. Qu, UV photochemical transformation kinetics of sulfonamides in aqueous solution based on optimized fluence quantification, Water Res. 75 (2015) 43-50.

[28] F. J. Real, F. J. Benitez, J. L. Acero, G. Roldan, F. Casas, Elimination of the emerging contaminants Amitriptyline hydrochloride, Methyl Salicylate, and 2‑Phenoxyethanol in purifiée water and secondary effluents by photolytic and radicalary Pathways, Ind. Eng. Chem. Res. 51 (2012) 16209–16215.

[29] M. J. García-Galán, C. E. Rodríguez-Rodríguez, T. Vicent, G. Caminal, M. S. Díaz Cruz, D. Barceló, Biodegradation of sulfamethazine by Trametes versicolor: removal from sewage sludge and identification of intermediate products by UPLC-QqTOF-MS, Sci. Total Environ. 409 (2011) 5505–5512.

[30] L.-C. Chuang, C.-H. Luo, C.-J Lin, Degradation Characteristics of Sulfaméthoxypyridazine in Water by Ozonation and Photocatalysis, Procedia Engineering 15 (2011) 5133–5137.

[31] F. J. Benitez, J. L. Acero, F. J. Real, G. Roldan, E. Rodriguez, Photochemical transformation of model emerging contaminants in ultra-pure water: Kinetics, by-products formation and degradation pathways, Water Res. 47 (2013) 870–880.

ACCEPTED MANUSCRIPT

Figures

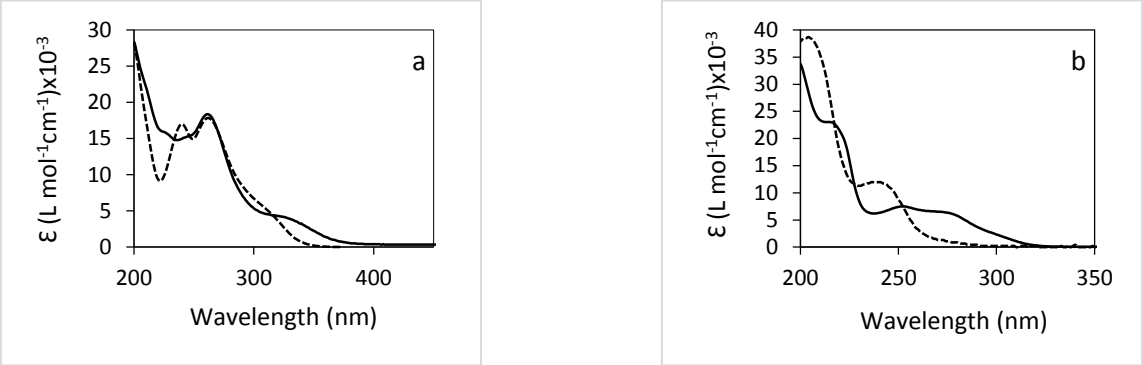

Fig. 1 UV-Vis absorption spectra in aqueous solution at pH 6.1 of (a) SMT (dashed line) and SMP (plain line), and (b) AMT (dotted line) and CMP (plain line).

ACCEPTED MANUSCRIPT

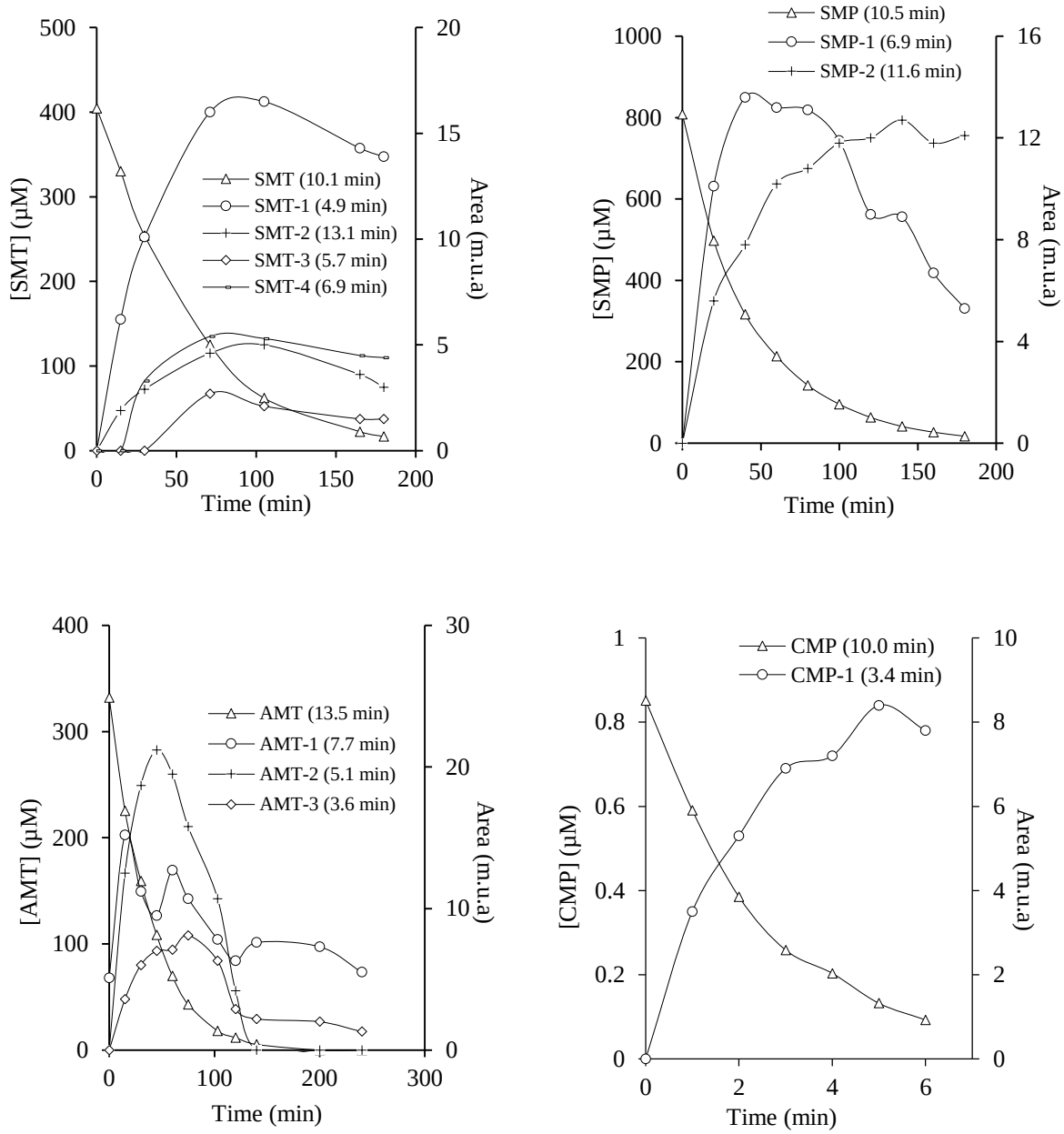

Fig. 2 Evolution of drug concentrations and of photoproduct areas as a function of irradiation (254 nm) time.

ACCEPTED MANUSCRIPT

Schemes

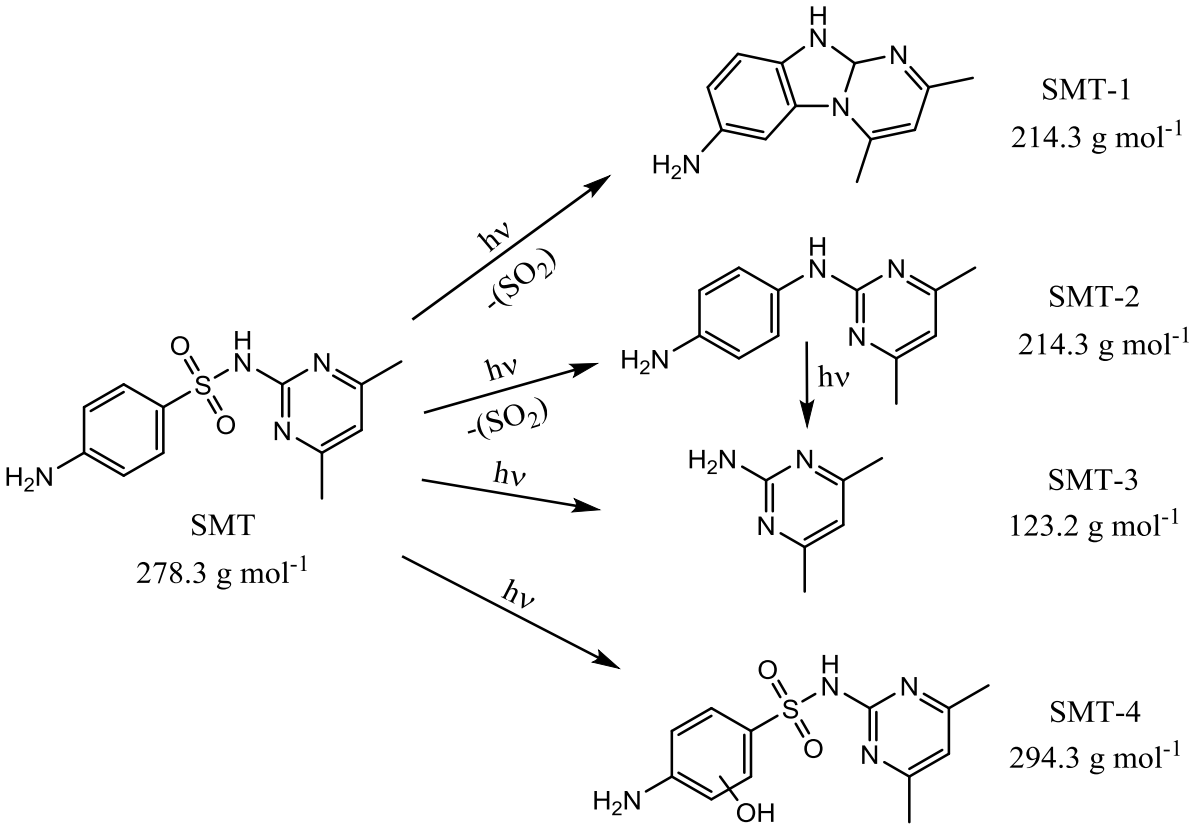

Scheme 1 Structures of SMT and of its products generated under UV irradiation in purified water.

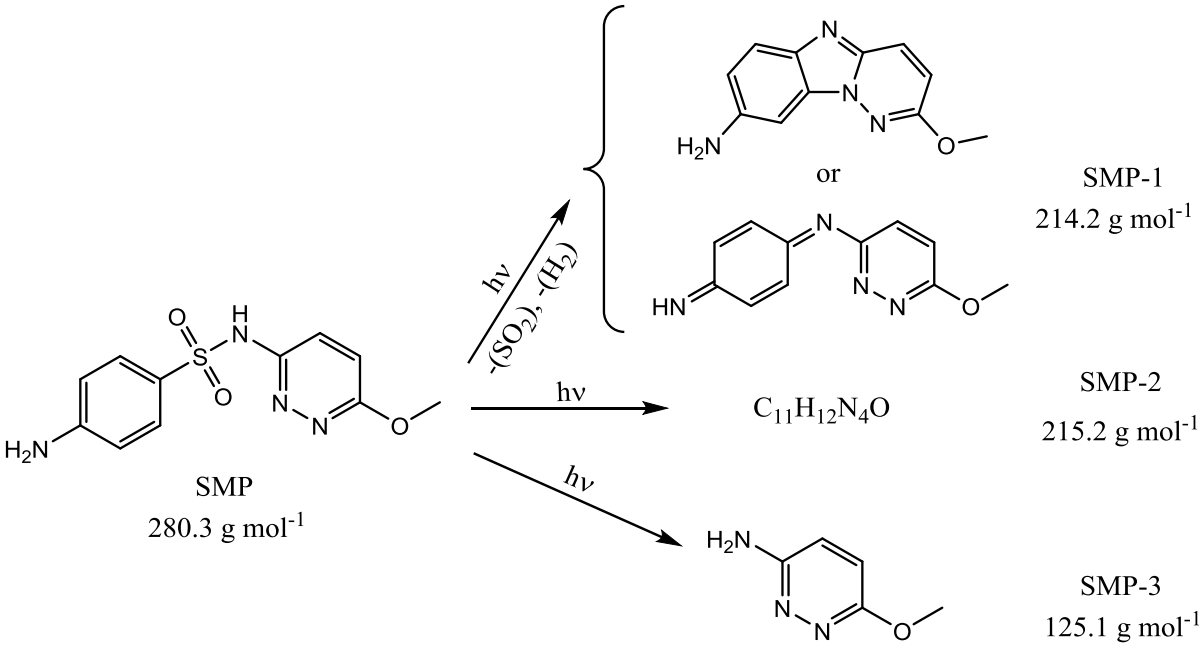

Scheme 2 Structures of SMP and of its products under UV irradiation in purified water.

ACCEPTED MANUSCRIPT

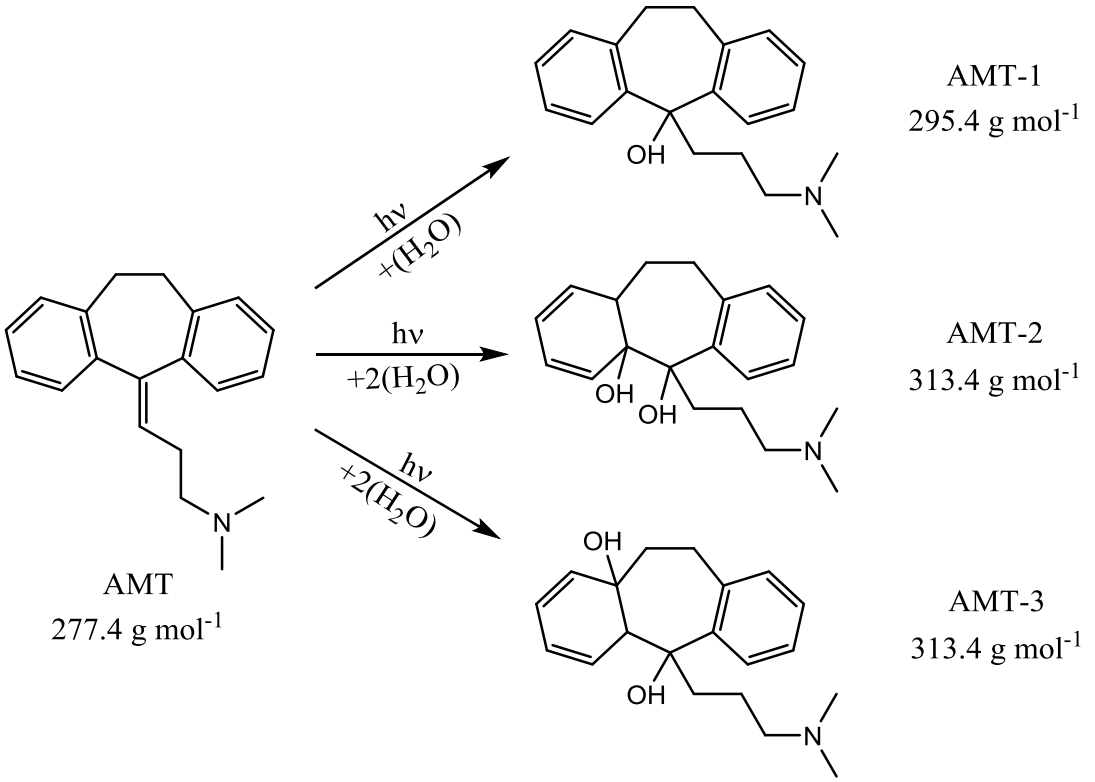

Scheme 3 Structures of AMT and of its products generated under UV irradiation in purified water.

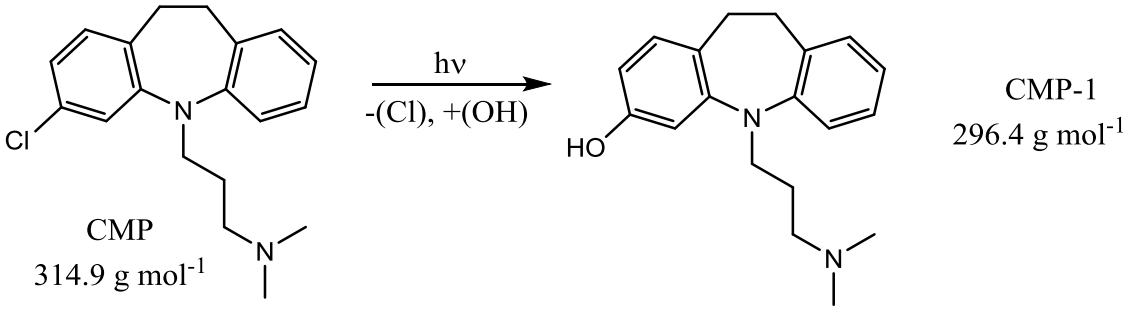

Scheme 4 Structures of CMP and of its product generated under UV irradiation in purified water.

ACCEPTED MANUSCRIPT

Tables

Table 1 First order degradation rate constants in purified (k_P, min^{-1}) and river (k_R, min^{-1}) waters obtained under simulated solar light irradiation. Quantum yields of photodegradation (ϕ_{254nm}), first order degradation rate constants (k_{UV}, min^{-1}) obtained under irradiation at 254 nm, and second order degradation rate constant (k_D, L mol^{-1} s^{-1}).

	$k_P \times 10^{-3}$	$k_R \times 10^{-3}$	$\phi_{254\,nm} \times 10^{-3}$	$k_{UV} \times 10^{-3}$	$k_D \times 10^{9}$
SMT	1.1 ± 1.1	3.7 ± 4.2	4.3 ± 0.1	57.3 ± 2.2	5.0 ± 0.1
SMP	0.9 ± 3.0	6.9 ± 5.0	5.1 ± 0.1	66.0 ± 1.3	5.0 ± 0.4
AMT	ND	ND	7.6 ± 0.2	39.9 ± 5.6	8.0 ± 0.3
CMP	18.2 ± 3.3	28.9 ± 2.4	65.0 ± 0.02	367.8 ± 30.1	9.5 ± 0.1

ND: not degraded

ACCEPTED MANUSCRIPT

Table 2 LC-MS/MS ESI+ analyses of SMT, SMP, AMT and CMP drugs and their photoproducts.

Name	m/z	Formula	Fragments (relative intensity)
SMT	279.1	$C_{12}H_{15}N_4O_2S$	
SMT-1	215.1	$C_{12}H_{15}N_4$	215 (100), 173 (10)
SMT-2	215.1	$C_{12}H_{15}N_4$	215 (100), 198 (20),108 (40)
SMT-3	124.1	$C_6H_{10}N_3$	124 (100), 107 (80), 82 (28), 67 (33)
SMT-4	295.1	$C_{12}H_{15}N_4O_3S$	295 (100), 186 (30), 124 (75)
SMP	281.0	$C_{11}H_{13}N_4O_3S$	
SMP-1	215.0	$C_{11}H_{11}N_4O$	215 (100), 200 (30), 183 (15), 145 (20)
SMP-2	216.1	$C_{11}H_{12}N_4O$	216 (100), 187 (20), 173 (15), 147 (12)
SMP-3	126.0	$C_5H_8N_3O$	126 (100), 111 (23)
AMT	278.1	$C_{20}H_{24}N$	
AMT-1	296.1	$C_{20}H_{26}NO$	296 (28), 278 (100)
AMT-2	314.2	$C_{20}H_{28}NO_2$	314 (100), 296 (25), 58 (12)
AMT-3	314.2	$C_{20}H_{28}NO_2$	314 (100), 270 (15)
CMP	315.1	$C_{19}H_{24}ClN_2$	
CMP-1	297.2	$C_{20}H_{25}N_2O$	86 (100), 58 (40)